

## **ATTACHED AND UNATTACHED ACTIVITY SIZE DISTRIBUTION OF SHORT-LIVED RADON PROGENY (<sup>214</sup>Pb) AND EVALUATION OF DEPOSITION FRACTION**

A. Mohamed, A. A. Ahmed, A. E. Ali, M. Yunes

*Physics Department, Faculty of Science, El-Minia University, El-Minia,  
Egypt Amermohamed6@hotmail.com*

### **ABSTRACT**

Inhalation of <sup>222</sup>Rn progeny in the domestic environment contributes the greatest fraction of the natural radiation exposure to the public. Dosimetric models are most often used in the assessment of human lung doses due to inhaled radioactivity because of the difficulty in making direct measurements. These models require information about the parameters of activity size distributions of radon progeny. The current study presents measured data on the attached and unattached activity size distributions of radon progeny in indoor air in El-Minia, Egypt. The attached fraction was collected using a low pressure Berner cascade impactor technique. A screen diffusion battery was used for collecting the unattached fraction. Most of the attached activities for <sup>222</sup>Rn progeny were associated with aerosol particles of the accumulation mode. The mean activity median aerodynamic diameter (AMAD) of this mode for <sup>214</sup>Pb was determined to be 401 nm with relative mean geometric standard deviation of 2.96. The mean value of specific air activity concentration of <sup>214</sup>Pb associated with that mode was determined to be  $4.74 \pm 0.44$  Bq m<sup>-3</sup>. The relative mean geometric standard deviations of unattached <sup>214</sup>Pb was determined to be 1.21 with the mean activity thermodynamic diameter (AMTD) of 1.2 nm. The mean unattached activity concentration of <sup>214</sup>Pb was found to be  $0.44 \pm 0.14$  Bq m<sup>-3</sup>. Based on the obtained results of radon progeny size distributions (unattached and attached), the deposition fractions in each airway generation of the human lung were evaluated by using a lung deposition model.

*Keywords: Deposition, size distribution, attached and unattached radon progeny*

### **INTRODUCTION**

Radon-222 is naturally occurring radioactive gas and decay product of <sup>226</sup>Ra. It is present in trace amounts in all rocks and soil. After the decaying of <sup>222</sup>Rn, the next members of the decay chain are <sup>218</sup>Po, <sup>214</sup>Pb, <sup>214</sup>Bi and <sup>214</sup>Po which are known as the short-lived decay products of radon. Radon and its decay products are found in variable concentrations indoors, outdoors, and in mining environments. It has been shown, since the 1960s, that occupational exposures to high concentrations of <sup>222</sup>Rn and its progeny have caused an increased risk of lung cancers. Since 1980s, the inhaled progeny of <sup>222</sup>Rn were recognized as the most important single contributor to internal radiation dosimetry. The infiltration of radon from the ground is usually the predominant source of indoor radon pollution<sup>(1)</sup>. High radon concentration in indoor air coupled with the prolonged exposure periods related to indoor habitation make

indoor radon a potential hazard <sup>(2)</sup>. Radon escapes from the ground and accumulates in rooms according to the strength of its emanation and its dilution by ventilation. Radon progeny are formed as positive ions or atoms, which are able to deposit on surfaces or attach to the particles of room air. This mechanism explained in Fig. 1. Depending on the geological location, house structure and ventilation rate, chronic exposure to indoor <sup>222</sup>Rn would be a health concern. The increased risks of lung cancers are associated with inhalation and deposition of short-lived radon progeny in the lung especially those of ultrafine progeny smaller than 2 nm, the so-called unattached fraction <sup>(3)</sup>.

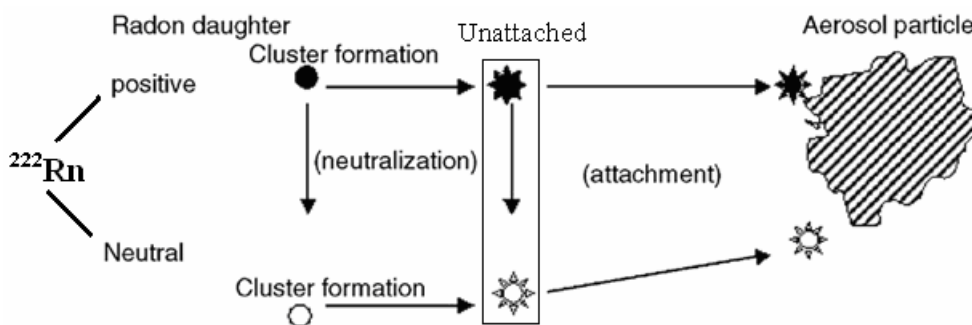


**Fig. 1:** Formation of radioactive aerosols.

The activity size distribution of radon progeny has been determined by tagging the natural aerosol particles with radon progeny. However, some measurements of activity size distribution have been performed in indoor air <sup>(4-21)</sup>. Most of these literatures indicate that the activity size distribution of the airborne radon progeny in the indoor environment consists of ultrafine clusters with median diameters below 4 nm (unattached activity) and radon progeny associated with ambient aerosol in the size range between 0.1 and 0.4  $\mu\text{m}$  (attached activity)<sup>(22)</sup>. Most of the unattached radon progeny is deposited in the respiratory tract during breathing, whereas 80% of the attached radon progeny are exhaled without deposition <sup>(23)</sup>. The unattached activity amounts up to about 10% of the total activity, but is considered to yield about 50% of the total radiation dose. Therefore, measurements of the unattached fraction are essential for the estimation of dose.

Inhalation of the short-lived radon progeny (<sup>218</sup>Po, <sup>214</sup>Pb, <sup>214</sup>Bi and <sup>214</sup>Po) makes the largest contribution to natural radiation exposure <sup>(24)</sup>. The unattached and attached radon progeny are deposited in different regions of the human respiratory tract due to the different particle sizes. Because the dose to lung tissues cannot be measured, a dosimetric model is necessary to estimate the radiation dose exposure. In all dosimetric models the calculated dose principally depends on activity concentration and the activity size distribution of the inhaled radioactive aerosol <sup>(24)</sup>.

Therefore, the first aim of the present study was summarized the measured data on the unattached and attached activity size distributions of <sup>214</sup>Pb as usually as the activity concentration of the same isotopes in indoor air. In addition, based on the obtained experimental data, the total deposition fraction has been calculated through the human lung by applying the deposition model of International Commission on Radiological Protection (ICRP) <sup>(25,26)</sup>.

## **MATERIALS AND METHODS**

### Instruments

#### Unattached size distribution

In the present work, a wire screen diffusion battery similar to that employed and calibrated by Cheng et al <sup>(27)</sup> was used. It was constructed with the same screen characteristics to determine the size distribution of unattached radon progeny. The diffusion battery consisted of five stainless-steel screens with 24, 35, 50, 200, and 635 mesh numbers. The screens were calibrated with monodisperse silver aerosol particles. The measured 50% cut-off diameters of the screens are 0.9, 1.3, 1.9, 4.0 and 7.9 nm.

The theory of this instrument is based on that the motion of very fine particles, in the diameter size range of about 2 nm, is strongly affected by random collisions with gas molecules. This is known as diffusion. A particle undergoing diffusion travels a random, irregular path. Its position at any given time depends on its most recent collision with a molecule. Therefore, some of these particles collide with the screen wires. Surface-attractive forces between particle and wire cause the particle to stick to the screen. Because of diffusion, a larger fraction of small particles will collide with the screen than of large particles.

#### **Attached size distribution**

A low pressure Berner cascade impactor was used to determine the activity size distribution of attached short-lived radon progeny (<sup>214</sup>Pb) <sup>(28)</sup>. It consisted of eight size fractionating stages and a back-up filter holder, and operated at a flow rate of 1.7 m<sup>3</sup> h<sup>-1</sup>. Aluminum foils were used as collection media and a glass fiber filter as the back up filter <sup>(29)</sup>. The collected activity on each impactor stage was measured with a well-type 3×3 NaI (TI) detector. Therefore, the collection efficiencies as well as the cut-off diameters of the impactor stage could be calculated. The measured 50% cut-off diameters were 82, 157, 270, 650, 1100, 2350, 4250 and 5960. The total interstage losses of aerosol particles were less than 2% of the total activity <sup>(28)</sup>.

The effect of the low pressure cascade impactor reduces the drag force on the particle. This reduction in drag allows smaller particle sizes to be collected in low pressure impactors compared with impactors which are operated at the normal pressure (sierra impactor). In that Impactor, an aerosol sample is drawn through a series of successively smaller nozzles consisting of round holes with a collection surface placed perpendicular to the direction of flow and very close to the exit of each nozzle. At each stage, the aerosol is accelerated in passage through the stage nozzle and the particles must make a right angle change of direction to follow the air streamlines; large particles are unable to negotiate the right-angle turn and impact upon the collector plate. The Impactor stages are designed to provide progressively higher jet speeds so that the average size of particles collected at each stage is successfully smaller. An efficient filter usually follows the final stage to collect all the smaller particles which successfully pass through the impactor.

## **Methods**

### **Unattached size distribution**

To determine the unattached activities of radon progeny, the aerosol attached and total radon progeny concentrations were measured. Each measurement consisted of two parallel samples: one with a single screen and the other as a reference sample without screen. This procedure was repeated with different screens. The screen was used only for collecting the unattached activities. The activities penetrating the screen (mostly attached to aerosol particle) and that of the reference sample were collected on membrane filters (Sartorius membrane filters type SM, 1.2 mm pore size, 25 mm diameter and an efficiency reaching about 100%) and the alpha activities were detected during and after air sampling by a surface barrier detector. According to the Ruffle method<sup>(30)</sup> and through utilizing  $^{241}\text{Am}$  as a radioactive source of alpha rays, the counting efficiency of the detector was found to be  $17.0 \pm 0.5\%$ . The detector has an active area of  $300 \text{ mm}^2$  and the separation between the filter and detector is 6 mm. With an energy resolution of about 300 KeV, it was possible to distinguish the alpha particle energies emitted during the decay of  $^{218}\text{Po}$  (6 MeV) and  $^{214}\text{Po}$  (7.69 MeV). In order to determine the activity concentrations of radon progeny ( $^{218}\text{Po}$ ,  $^{214}\text{Pb}$  and  $^{214}\text{Po}$ ), the measurements were performed in two steps. Firstly, the alpha particle spectrum was collected during a sampling period of 30 min. Secondly, after waiting for a time period of 30 min without sampling, the alpha particle spectrum was measured again (during decay) for a time period of 30 min. From the measured alpha counts of  $^{218}\text{Po}$  and  $^{214}\text{Po}$  during the sampling period and the  $^{214}\text{Po}$  counts during the decay period, the activity concentrations of  $^{218}\text{Po}$ ,  $^{214}\text{Pb}$  and  $^{214}\text{Po}$  could be calculated according to a method described by Wicke<sup>(31)</sup>. The attached activities were derived from the sample obtained with the screen. The collected unattached activity on the screen is the difference between the measurements of the reference sample (without screen) and the screen sample.

The parameters of unattached activity size distribution, Active Median Thermodynamic Diameter (AMTD) and Geometric Standard Deviation (GSM), were obtained from a graphical cumulative method. The cumulative unattached activity concentration fraction was plotted versus the cut-off diameter of the screens. AMTD is defined as the diameter at 50% cumulative fractions. GSM of the size distribution is defined as the diameter at 84% cumulative activity divided by the diameter obtained at 50%.

### **Attached size distribution**

For determination of the size distribution of the attached radon progeny ( $^{214}\text{Pb}$ ) with the low-pressure Berner impactor, several runs were conducted at different times. After air sampling, the foils were pressed into pellets and the relative gross  $\gamma$ -ray emitting activities on each impactor stage were measured with a well-type  $3 \times 3$  NaI(Tl) detector connected to a multichannel analyzer. The parameters of the attached activity size distribution, Active Median Aerodynamic Diameter (AMAD) and Geometric Standard Deviation (GSM), were obtained by the same method which was explained for unattached activity size distribution.

The measured data of unattached as well as attached  $^{214}\text{Pb}$  were applied to the dosimetric lung model of International Commission on Radiological Protection<sup>(26)</sup> for calculating the total deposition fraction to the human respiratory tract. The deposition

was evaluated for a unit density of spherical particles and a ventilation rate of 1 m<sup>3</sup> h<sup>-1</sup> (light work), for adult male.

### RESULTES AND DISCUTIONS

From Table 1, the unattached AMTD for <sup>214</sup>Pb ranged from 1.1 to 1.3 nm with a mean value of 1.2 nm and with relative GSD of 1.21 (range from 1.19 to 1.32 nm). The mean activity concentration of unattached <sup>214</sup>Pb was found to be 0.44 ± 0.14 Bq m<sup>-3</sup> (range from 0.04 to 1.5 Bq m<sup>-3</sup>). The activity size distribution of the unattached fraction of <sup>214</sup>Pb is shown in Fig. 2. The unattached activity fractions are plotted as histograms against the cut-off diameter of the screens. For the single screen with a cut-off diameter of 7.9 nm, no unattached activities are observed. This may be because the maximum size (5 nm) of the unattached fractions is below the cut-off diameter of this screen.

DB			IM		
Unattached parameters of <sup>214</sup> Pb			Attached parameters of <sup>214</sup> Pb		
AMTD(nm)	GSD	C (Bq m <sup>-3</sup> )	AMAD(nm)	GSD	C* (Bq m <sup>-3</sup> )
1.2 (1.1 - 1.3)	1.21 (1.19 - 1.32)	0.44 ± 0.14 (0.04 - 1.5)	401 (344 - 525)	2.96 (2.4 - 3.5)	4.74 ± 0.44 (3.6 - 6.3)

**Table 1** represents the experimental results as, mean activity median thermodynamic diameter (AMTD), relative geometric standard deviation (GSD) and activity concentration (C) of unattached <sup>214</sup>Pb. And mean activity median aerodynamic diameter (AMAD), relative geometric standard deviation (GSD) and specific air activity concentration (C\*) of attached <sup>214</sup>Pb, which were carried out in indoor air of El-Minia University, El-Minia, Egypt

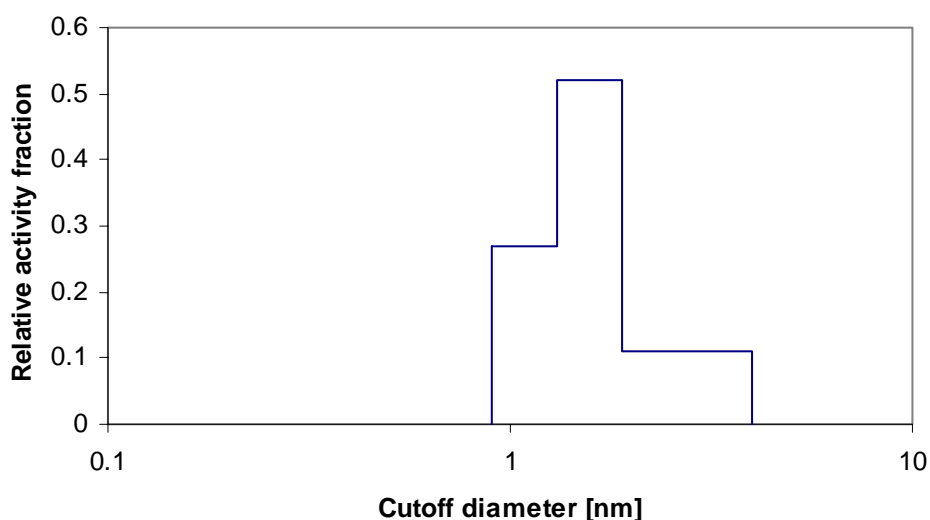


**Fig. 2:** Activity size distribution of unattached [<sup>214</sup>Pb] in indoor air.

The attached activity size distributions of radon progeny ( $^{214}\text{Pb}$ ) which was measured by Berner cascaded impactor in indoor air are summarized in Table 1. The attached AMAD of the  $^{214}\text{Pb}$  varied between 344 and 525 nm with a mean value of 401 nm and a mean GSD of 2.96 (range from 2.4 to 3.5 nm). The specific air activity concentrations of attached  $^{214}\text{Pb}$  were found to vary between 3.6 and 6.3  $\text{Bq m}^{-3}$  with a mean value of  $4.74 \pm 0.44 \text{ Bq m}^{-3}$ . The activity size distribution of the attached fraction of  $^{214}\text{Pb}$  is shown in Fig. 3. The attached activity fractions are plotted as histograms vs the cut-off diameters of the stages.

Because the measurements were performed on different times, considerable fluctuations in the size distributions were observed. Also, according to meteorological conditions sometimes very small activities in the coarse mode (aerosol size range < 2000 nm) were measured. Most of the derived activity size distributions could be approximated as unimodal log-normal distributions represented by the accumulation mode (100 nm < aerosol particle size < 2000 nm). This may be traced to the removal processes of large particles, which are controlled by the dry deposition. The deposition velocity of particle in the accumulation mode is about  $10^{-2} \text{ cm s}^{-1}$  (32). Particle with such deposition velocity are very slowly removed and therefore their residence time are relatively long. On the other hand, the deposition velocity of particles in the coarse mode (< 2000 nm) extends to  $20 \text{ cm s}^{-1}$  (32) which is very high in comparison with that of accumulation mode particles. Therefore, the residence time of the particles in the coarse mode is very short and so it will be not enough chance for these particles to coagulate for producing a broad size distribution of the coarse mode.

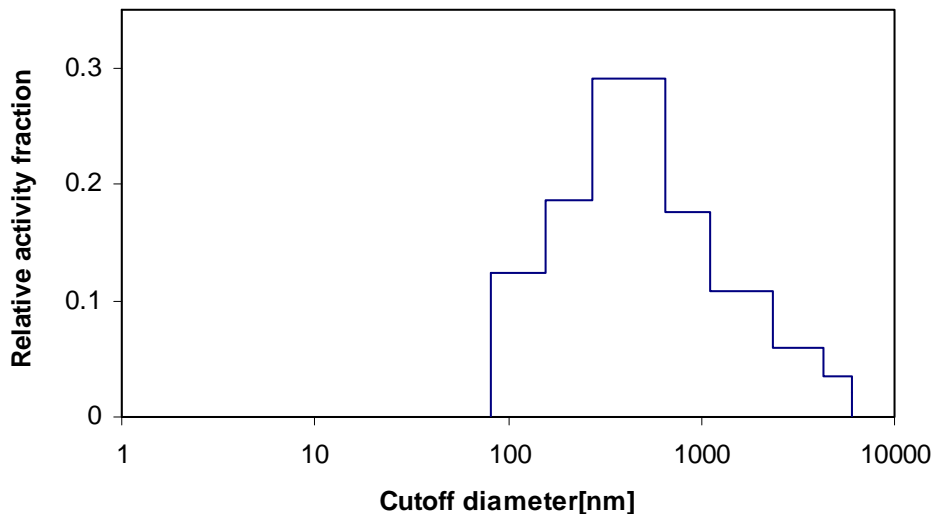


**Fig. 3:** Activity size distribution of attached [ $^{214}\text{Pb}$ ] in indoor air.

With the Berner impactor, Hopke et al (5) measured the activity median aerodynamic diameter of 200-500 nm in indoor air. Reineking et al. (4,7) have published an indoor size distribution with activity median aerodynamic diameter of 188 nm and 238 nm respectively, which is a factor of two smaller than the present value. The relative deviation between the present value and that given in the literature may be attributed to the difference in the sampling locations and weather conditions. As it is known the radon progeny is strongly affected by the temperature and relative humidity.

Based on the parameters of activity size distribution of  $^{214}\text{Pb}$  (see Table 1), the total deposition fraction of  $^{214}\text{Pb}$  has been calculated using the deposition model of ICRP <sup>(26)</sup>. The total deposition fraction through the human lung was found to be 98% for unattached fraction and 32% for attached fraction.

## CONCLUSIONS

From what has been discussed throughout this work, the following conclusions are reached:

1. Most of the attached activities are associated with the accumulation mode.
2. The AMAD of 401 nm was determined for attached radionuclide  $^{214}\text{Pb}$  with the GSD of 2.96.
3. The AMTD value of the unattached fraction of  $^{214}\text{Pb}$  was found to be 1.2 nm with the GSD 1.21.
4. The deposition fraction of attached radon progeny, in the environment studied, is lower than that of unattached progeny. This clears the disproportionately large contributions to the dose from exposure to small fraction of radon progeny in the unattached state <sup>(33)</sup>.

## REFERENCES

- [1] Neznal, M. and Smarda, J. Radon Risk Classification of Foundation Soils: Some Remarks. In: *Proceedings of the Symposium on Radiation Protection in Neighbouring Countries in Central Europe*, Portoroz, Slovenia, 63-65 (1995).
- [2] Marcinowski, F. M., Nationwide Survey of Residential Radon Levels in the US, *Radiat. Prot. Dosim.* 45, 419-424 (1992).
- [3] Hopke, P. K. Some Thoughts on the Unattached Fraction of Radon Decay Products. *Health Phys.* 63, 209-212 (1992).
- [4] Reineking, A., Becker, K. H. and Porstendörfer, J., Measurements of Activity Size Distributions of the Short-Lived Radon Daughters in the Indoor and Outdoor Environment, *Radiat. Prot. Dosim.* 24, 245-250 (1988).
- [5] Hopke, P. K., Ramamurthi, M. and Li, C. S. Measurement of the Size Distributions of Radon Progeny in Indoor Air. In *Aerosol: Science, Industry, Health and Environment*, Masuda, S and Takashi, K., eds, Vol. 2, Pergamon Press, Ltd, Oxford, 842-847 (1990).
- [6] Tu, K. W., Knutson, E. O. and George, A. C., Indoor Radon Progeny Aerosol Size Measurements in Urban, Suburban, and Rural Regions, *Aerosol Sci. Technol.* 15, 170-178 (1991).
- [7] Reineking, A., Knutson, E. A., George, A. C., Solomon, S. B., Kesten, J., Butterweck, G. and Porstendörfer, J. Size Distribution of Unattached and Aerosol-Attached Short-Lived Radon Decay Products: Some Results of Intercomparison Measurements, *Radiat. Prot. Dosim.* 56, 113-118 (1994).
- [8] Papastefanoy, C. and Ioannidou, A. Activity Size Distribution of Radioactive Aerosols in the Atmosphere. *J. Aerosol Sci.* 29, 569-570 (1998).
- [9] Reineking, A., Porstendörfer, J., Dankelmann, V. and Wendt, J. The Size Distribution of the Unattached Short-lived Radon Decay Products, *Radioaktivität in Mensch und Umwelt*, Band I, 503-508, Publication Series: Progress in Radiation Protection, ISSN 1013-4506 (in German), (1998).

- [10] Harley, N. H., Chittaporn, P., Fisenne, I. M. and Perry, P. <sup>222</sup>Rn Decay Products as Tracers of Indoor and Outdoor Aerosol Particle Size. *J. Environ. Radioact.* 51, 27-35 (2000).
- [11] Porstendörfer, J., Zock, C. and Reineking, A. Aerosol Size Distribution of the Radon Progeny in Outdoor Air. *J. Environ. Radioact.* 51, 37-48 (2000).
- [12] Shimo, M. and Saito, H. Size Distribution of Radon Progeny Aerosols in Indoor and Outdoor Air. *J. Environ. Radioact.* 51, 49-57 (2000).
- [13] Cheng, Y. S., Chen, T. R., Yeh, H. C., Bigu, J., Holub, R., Tu, K., Knutson, E. O. and Falk, R. Intercomparison of Activity Size Distribution of Thoron Progeny and a Mixture of Radon and Thoron Progeny. *J. Environ. Radioact.* 51, 59-78 (2000).
- [1] Cavallo, A. J. Understanding Mine Aerosols for Radon Risk Assessment. *J. Environ. Radioact.* 51, 99-119 (2000).
- [14] Porstendörfer, J. Physical Parameters and Dose Factors of the Radon and Thoron Decay Products. *Radiat. Prot. Dosim.* 94, 365-373 (2001).
- [1] Porstendörfer, J. Influence of Physical Parameters on Doses from Radon Exposures. *Int. Congr. Ser.* 1225, 149-160 (2002).
- [15] Kendall, G. M. and Smith, T. J. Doses to Organs and Tissues from Radon and Its Decay Products. *J. Radiol. Prot.* 22, 389-406 (2002).
- [1] Yamasaki, K., Oki, Y., Yamada, Y., Tokonami, S. and Iida, T. Optimization of Measuring Methods on Size Distribution of Naturally Occurring Radioactive Aerosols. *Int. Congr. Ser.* 1276, 297-298 (2005).
- [16] Mohamed, A. Influence of Radioactive Aerosol and Biological Parameters of Inhaled Radon Progeny on Human Lung Dose, *Radiat. Prot. Dosim.* 113, 115-122 (2005).
- [17] Vaupotič, J. Nano-Size Radon Short-Lived Progeny Aerosols in Slovenian Kindergartens in Winter time. *Chemosphere* 69, 856-863 (2007).
- [18] Michielsen, N. and Tymen, G. Semi-Continuous Measurement of the Unattached Radon Decay Products Size Distributions from 0.5 to 5 Nm by an Array of Annular Diffusion Channels. *J. Aerosol Sci.* 38, 1129-1139 (2007).
- [19] Butterweck-Dempewolf, G., Shuler, Ch. and Vezzu, G. Size Distribution of the Unattached Fraction of Radon Progeny. In: *Proc. Eur. Conf. on Protection against Radon at Home and at Work*. Praha, Czech Republic, 28-32 (1997).
- [20] James, A. C., Gehr, P., Masse, R., Cuddihy, R. G., Cross, F. T., Birchall, A., Durham, J. S. and Briant, J. K. Dosimetry Model for Bronchial and Extrathoracic Tissues of the Respiratory Tract. *Radiat. Prot. Dosim.* 37, 221-230 (1991).
- [21] Zock, C., Porstendörfer, J. and Reineking, A. The Influence of Biological and Aerosol Parameters of Inhaled Short-Lived Radon Decay Products on Human Lung Dose. *Radiat. Prot. Dosim.* 63, 197-206 (1996).
- [22] NRPB-SR264, 1993 NRPB-SR264, LUDEP 1.0: Personal computer program for calculating internal doses using the new ICRP respiratory tract model, Pacific Northwest laboratory, Richland, Washington, USA (1993).
- [23] ICRP Human Respiratory Tract Model for Radiological Protection. Oxford: Pergamon Press, Publication 66 (1994).
- [24] Cheng, Y. S., Su, Y. F., Newten, G. J. and Yeh, H. C. Use of a Graded Diffusion Battery in Measuring the Activity Size Distributions of Thoron Progeny, *J. Aerosol Sci.* 23, 361-372 (1992).
- [25] Reineking, A., Scheibel, H. G., Hussin, A., Becker, K. H. and Porstendörfer, J. Measurements of Stage Efficiency Functions Including Interstage Losses for Sierra and Berner Impactor and Evaluation of Data by Modified Simplex Method. *J. Aerosol Sci.*, 15, 376-380 (1984).

- [26] Lurzer, C. Über die Bestimmung von Multimodalen Grossenverteilungen Atmosphärischer Aerosole. *Mittels unterdrückkaskaden impaktoren, Dissertation*, Wien, Austria (1980).
- [27] Ruffle, M. P. The Geometrical Efficiency of a Parallel Disc-Source and Detector System. *Nucl. Instr. Meth.* 52, 354-356 (1967).
- [28] Wicke, A. Untersuchungen zur Frage der Natürlichen Radioaktivität der Luft in Wohn und Aufenthaltsräumen. *Ph.D. Thesis, University Giessen*, Germany (1979).
- [29] Ahmed, A. A. Untersuchungen zur Aerosoldeposition an Oberflächen. *Ph.D. Thesis, University Giessen*, Germany (1979).
- [30] National Research Council (NRC). Comparative Dosimetry of Radon in Mines and Homes. (Washington, DC: National Academy Press) (1991).